Structure of YciA from *Haemophilus influenzae* (HI0827), a Hexameric Broad Specificity Acyl-Coenzyme A Thioesterase[†,‡]

Mark A. Willis,[§] Zhihao Zhuang,[△] Feng Song,[△] Andrew Howard,[⊥] Debra Dunaway-Mariano,[△] and Osnat Herzberg*[,§]

Center for Advanced Research in Biotechnology, W. M. Keck Laboratory for Structural Biology, University of Maryland Biotechnology Institute, Rockville, Maryland 20850, Department of Chemistry, University of New Mexico, Albuquerque, New Mexico 87131, and Biological, Chemical, and Physical Sciences, Illinois Institute of Technology, Chicago, Illinois 60616

Received November 26, 2007; Revised Manuscript Received January 9, 2008

ABSTRACT: The crystal structure of HI0827 from *Haemophilus influenzae* Rd KW20, initially annotated "hypothetical protein" in sequence databases, exhibits an acyl-coenzyme A (acyl-CoA) thioesterase "hot dog" fold with a trimer of dimers oligomeric association, a novel assembly for this enzyme family. In studies described in the preceding paper [Zhuang, Z., Song, F., Zhao, H., Li, L., Cao, J., Eisenstein, E., Herzberg, O., and Dunaway-Mariano, D. (2008) *Biochemistry 47*, 2789−2796], HI0827 is shown to be an acyl-CoA thioesterase that acts on a wide range of acyl-CoA compounds. Two substrate binding sites are located across the dimer interface. The binding sites are occupied by two CoA molecules, one with full occupancy and the second only partially occupied. The CoA molecules, acquired from HI0827-expressing *Escherichia coli* cells, remained tightly bound to the enzyme through the protein purification steps. The difference in CoA occupancies indicates a different substrate affinity for each of the binding sites, which in turn implies that the enzyme might be subject to allosteric regulation. Mutagenesis studies have shown that the replacement of the putative catalytic carboxylate Asp44 with an alanine residue abolishes activity. The impact of this mutation is seen in the crystal structure of D44A HI0827. Whereas the overall fold and assembly of the mutant protein are the same as those of the wild-type enzyme, the CoA ligands are absent. The dimer interface is perturbed, and the channel that accommodates the thioester acyl chain is more open and wider than that observed in the wild-type enzyme. A model of intact substrate bound to wild-type HI0827 provides a structural rationale for the broad substrate range.

The acyl-coenzyme A (CoA)[1] thioesterases are important metabolic and regulatory enzymes in all living systems. A subclass of acyl-CoA thioesterases adopts a fold termed "hot dog", which was first described in the structure of another enzyme acting on a thioester, the β-hydroxydecadecanoyl thiol ester dehydrase (FabA) from *Escherichia coli* (*1*). The hot dog fold consists of a central long α-helix wrapped in a β-sheet. Most known members of this family associate into dimers with the active sites located at the dimer interface, and these dimers may further associate into higher oligomeric forms.

When we began structural and functional studies, HI0827 from *Haemophilus influenzae* (homologue of YciA from *E. coli*) was a member of a protein sequence family of unkown function, which was only 14% identical in sequence with the *Arthrobacter* 4-hydroxybenzoyl-CoA thioesterase, a tetrameric protein exhibiting the hot dog fold, yet the likely relationship between the two proteins was detected by five iteration cycles of PSI-BLAST (*2*). Currently, one cycle of PSI-BLAST detects 575 family members of the HI0827 clade in the nonredundant sequence database (*E* score cutoff of 10^{-3}). However, to the best of our knowledge, none of these other clade members have been subjected to structure–function analysis.

The studies of HI0827 function, and the function of its close sequence homologue YciA from *E. coli* (69% amino acid identity), are reported in the preceding paper (*3*). Briefly, we found that these two cytoplasmic enzymes display high catalytic efficiency in the hydrolysis of a wide range of acyl-CoA metabolites, including long chain fatty acyl-CoAs. CoA serves as a strong feedback inhibitor, which we suggest may serve to regulate activity in the cell.

The location of the HI0827 gene within a cluster of genes related to cell wall processes suggested that it might be a representative of a new functional class of thioesterases. HI0827 shares an operon with HI0828, a protein whose structure was determined previously, but its function remains

[†] Supported by National Institutes of Health Grants P01 GM57890 (O.H.) and RO1 GM28688 (D.D.-M.).

[‡] Protein Data Bank coordinates and structure factors have been deposited as entries 1YLI (wild-type HI0827) and 3BJK (D44A mutant HI0827).

* To whom correspondence should be addressed: Center for Advanced Research in Biotechnology, 9600 Gudelsky Dr., Rockville, MD 20850. Telephone: (240) 314-6245. Fax: (240) 314-6255. E-mail: osnat@carb.nist.gov.

[§] University of Maryland Biotechnology Institute.

[△] University of New Mexico.

[⊥] Illinois Institute of Technology.

[1] Abbreviations: CoA, coenzyme A; K^+Hepes, potassium salt of *N*-(2-hydroxyethyl)piperAzine-*N*′-2-ethanesulfonate; PCR, polymerase chain reaction; PEG, polyethylene glycol; Bicine, *N*,*N*-bis(2-hydroxyethyl)glycine; MAD, multiwavelength anomalous diffraction; rmsd, root-mean-square deviation; PDB, Protein Data Bank.

10.1021/bi702336d CCC: $40.75
Published on Web 02/09/2008

unknown (*4*). To complement the biochemical characterization of HI0827 and to explore the structural variations within the acyl-CoA thioesterase family, we have undertaken a crystallographic analysis. Indeed, the study revealed a new structural class of hexameric hot dog thioesterases.

METHODS

Protein Production. Wild-type HI0827 from *H. influenzae* Rd KW20 was cloned, expressed, and purified as described in the preceding paper (*3*). Site-directed mutagenesis was carried out using a PCR-based strategy (*5*) with the wild-type HI0827 gene (as template), commercial primers, the PCR kit supplied by Stratagene, and the Power Block IITM System thermal cycler manufactured by ERICOMP. PCR-amplified DNAs were cloned into the pET-23b vector (Novagen) for expression in *E. coli* BL21(DE3). The mutated genes were verified by DNA sequencing. HI0827 mutant proteins D44A and N29A were purified by the same procedure as the wild-type protein and shown to be homogeneous by sodium dodecyl sulfate−polyacrylamide gel electrophoresis analysis. The yields of D44A and N29A HI0827 are 45 and 50 mg of protein/g of wet cells, respectively.

Structure Determination. Crystals of HI0827 were grown at room temperature by the vapor diffusion method in hanging drops using equal volumes of protein solution [15 mg/mL protein in 10 mM K^+Hepes (pH 7.5) and 150 mM KCl] and reservoir solution [10% PEG 4000, 100 mM Bicine (pH 8), and 200 mM calcium acetate]. Crystals belonging to space group $I4_132$ grew within a few days. They were cryoprotected by the slow addition (over a couple hours) of increasing amounts of glycerol (up to 18%) to crystal-containing drops, which were adjusted to contain 12% PEG 4000. This addition of glycerol was performed under a thin coating of perfluoropolyether oil (MW = 2800; Aldrich). Crystals were then flash-cooled in liquid propane at liquid nitrogen temperature. The D44A HI0827 mutant was also crystallized in hanging drops [16 mg/mL protein in 10 mM K^+Hepes (pH 7.5) and 150 mM KCl] using 30% saturated sodium citrate, 100 mM K^+Hepes (pH 7.5), and 5% ethylene glycol. The crystals belonged to space group $P2_1$. They were cryoprotected using ethylene glycol in place of glycerol following the same procedure as described for the wild-type enzyme crystals.

Wild-type HI0827 diffraction data were collected on IMCA-CAT beamline 17-ID at the Advanced Photon Source (Argonne National Laboratory, Argonne, IL). In addition to native data, a multiwavelength anomalous diffraction (MAD) data set was collected at the L_{III} absorption edge of platinum (λ = 1.0723 Å) on a crystal grown and cryoprotected in the same manner as the native crystal with the exception that prior to being flash-cooled the crystal was soaked for 18 h in a cryosolution augmented with 1.5 mM K_2PtCl_4. Diffraction data for the D44A HI0827 mutant were collected on the home facility using Cu Kα radiation generated by a MicroMax-007 rotating anode X-ray generator equipped with an R-Axis IV^{++} detector (Rigaku-MSC).

Wild-type HI0827 diffraction data were processed with the HKL suite (*6*) and scaled with SOLVE (*7*) (Table 1). The MAD data to 2.3 Å resolution were used in SOLVE to identify six platinum sites. The resulting phases were extended to 2.0 Å resolution and improved with the use of 2-fold noncrystallographic symmetry and density modification as implemented in RESOLVE (*8*). The two molecules in the asymmetric unit were partially built using the automatic tracing option in RESOLVE and completed by manual building on an interactive graphics workstation using O (*9*). Refinement of the model (truncating the data at 1.95 Å resolution because of the rapid deterioration in diffraction quality between 1.95 and 1.90 Å) was performed using CNS (*10*) followed by REFMAC (*11*) as implemented in CCP4 (*12*), with four TLS groups (*13*) to yield an overall *R*-factor of 0.184 and an R_{free} of 0.227 (Table 1). The final model includes two protein molecules, two CoA molecules (one at half-occupancy), two glycerol molecules, four calcium ions (present in the crystallization solution), and 215 water molecules.

The D44A HI0827 data were processed and scaled using CrystalClear (Rigaku MSC Inc.). The wild-type structure served as the search model for molecular replacement using CNS (*10*). The D44A mutant HI0827 structure, containing a complete hexamer in the asymmetric unit, was refined using REFMAC. Eight TLS groups were used along with riding hydrogens to yield a final *R*-factor of 0.172 and an R_{free} of 0.210 for data to a resolution of 1.9 Å (Table 1). One of the hexamer's subunits (chain F in the PDB entry) has three disordered residues that are not modeled (residues 130, 137, and 138). In addition to the six protein molecules, the final model of D44A HI0827 includes three citrate molecules, 28 ethylene glycol molecules, and 463 water molecules.

Model geometry was evaluated using Procheck (*14*) and WHAT_CHECK (*15*) (Table 1). The dihedral angles of all residues are within the allowed region of the Ramachandran plot. Accessible surface area was calculated using GRASP (*16*), and figures were prepared with PyMOL (DeLano Scientific), MOLSCRIPT (*17*), and RASTER3D (*18*).

Steady State Kinetic Constant Determinations. The steady state kinetic constants of wild-type and mutant HI0827-catalyzed hydrolyses of isobutyryl-CoA and lauroyl-CoA were determined using the same protocol described in the preceding paper (*3*).

RESULTS AND DISCUSSION

Overall Fold and Oligomeric Association. The structure of the 17 kDa wild-type protein YciA from *H. influenzae* (HI0827) was determined at 1.95 Å resolution and used as a search model to determine the structure of the D44A HI0827 mutant by molecular replacement. HI0827 adopts the dimeric hot dog fold seen in previously reported structures of acyl-CoA thioesterases (*19–21*), but unlike most previous structures, it assembles into hexamers (Figure 1). The protomer structure consists of a five-stranded β-sheet that cradles a central α-helix and packs against an external C-terminal α-helix. In crystals of the wild-type protein, the two polypeptide chains comprise the asymmetric unit. They are very similar to one another at 0.3 Å root-mean-square deviation (rmsd) for the C_α atoms of residues 11–152. They differ in their N-termini, where one molecule contains five more ordered residues than the second molecule. The β-sheets of the two protomers associate to form a 10-stranded β-sheet cradling the two central α-helices, one from each

Table 1: Crystallographic Data and Refinement Statistics for HI0827

Data Collection		
	wild-type	D44A
space group	$I4_132$	$P2_1$
cell dimensions	$a = b = c = 163.7$ Å	$a = 78.5$ Å, $b = 63.1$ Å, $c = 104.7$ Å; $\beta = 100.1°$
no. of molecules per asymmetric unit	2	6

	wild-type	λ_1 Pt peak	λ_2 Pt edge	λ_3 Pt remote	D44A
wavelength (Å)	1.5545	1.0720	1.0723	1.0543	1.5418
resolution (Å)	30–1.9	25–1.95	25–1.95	25–2.0	30–1.9
no. of observations	578005	1118308	1129318	1054970	485015
no. of unique reflections[a]	29132	51723	51690	47955	79693
completeness (%)[b]	98.3(83.4)	99.8 (100)	99.8 (100)	99.7 (100)	98.0(96.4)
R_{merge} (I)[b,c]	0.075(0.65)	0.107(0.699)	0.110(0.752)	0.108(0.583)	0.065(0.383)
$\langle I/\sigma(I)\rangle$	17.0(2.0)	13.3(5.1)	12.9(4.7)	13.3(5.9)	8.2

Refinement		
	wild-type	D44A
resolution (Å)	1.95	1.90
wavelength (Å)	1.5545	1.5418
no. of unique reflections ($F > 0$)	26684	71724
completeness (%)	97.2	99.9
$R_{overall}$[d]	0.184	0.172
R_{free}[d]	0.227	0.210
no. of protein atoms	2195	6368
no. of water molecules	215	463
no. of other atoms	112	139
rmsd from ideal geometry		
bond lengths (Å)	0.017	0.019
bond angles (deg)	1.6	1.7
Ramachandran plot (%)[e]		
most favored/allowed	92.1/7.9	93.2/6.8
generously allowed/disallowed	0.0/0.0	0.0/0.0
average B factor (Å^2)		
protein	35.3	34.5
water	37.1	37.9
other atoms	34.1	39.6

[a] Pt data Bijvoet pairs are treated as independent reflections. [b] For reflections with $I > 0$. Values in parentheses are for the highest-resolution shell. [c] $R_{merge} = \sum_{hkl}[(\sum_j |I_j - \langle I\rangle|)/\sum_j I_j|]$. [d] $R_{overall} = \sum_{hkl}\triangle F_{obs}| - k|F_{calc}\triangle_{hkl}|F_{obs}|$, calculated for all reflections. R_{free} is calculated for a randomly selected 8% set of reflections not included in the refinement. [e] Analyzed using ProCheck (*14*).

protomer. The dimer interface buries 1810 Å^2 of accessible surface area.

The molecules pack in the crystal as a trimer of dimers (Figure 1B), consistent with the hexameric oligomerization obtained from sedimentation equilibrium experiments (see ref *3*). The hexameric association leads to burial of a total of 10642 Å^2 of accessible surface area. In addition to HI0827, two bacterial homologous proteins (~20% identical sequence) whose structures have been determined by structural genomics centers also form hexamers: the proteins from *Bacillus halodurans* (PDB entry 1VPM deposited by the Joint Center for Structural Genomics) and *Bacillus cereus* (PDB entry 1Y7U deposited by the Midwest Center for Structural Genomics). The N-terminal domain of acyl-CoA thioesterase 7 from mouse (*22*) and the C-terminal domain of acyl-CoA thioesterase 7 from human (PDB entry 2QQ2 deposited by the Structural Genomics Consortium) are also hexameric, although they do not exhibit significant sequence similarity to HI0827. The two-domain fusion hot dog fold protein from *Agrobacterium tumefaciens* (PDB entry 2GVH deposited by the Joint Center for Structural Genomics) is trimeric. With the exception of one structure, all other reported structures within this hot dog fold of the acyl-CoA thioesterase family are tetrameric, comprising either β-sheets that pack against one another to form the tetramer [viz. 4-hydroxybenzoyl CoA thioesterase from *Arthrobacter* sp. strain SU (*21*)] or β-sheets that are located on the outside of the tetrameric complex [viz. 4-hydroxybenzoyl CoA thioesterase from *Pseudomonas* sp. strain CBS-3 (*19*)]. *E. coli* thioesterase II is similar to the *Arthrobacter* enzyme except that as with the *A. tumefaciens* enzyme, two hot dog fold domains comprise a subunit (*20*). In addition, a putative thioesterase consisting of a single dimeric hot dog fold has been described (*23*). Interestingly, the structures of β-hydroxyacyl(acyl carrier protein) dehydratase (FabZ) from *Pseudomonas aeruginosa* and from *Plasmodium falciparum* exhibit the hot dog fold with a trimer of dimers association, but the assembly is different from that of the hexameric acyl-CoA thioesterases, with the dimers rotated relative to the 3-fold symmetry axis by approximately 90° (*24, 25*).

The structure of the D44A HI0827 mutant, with the entire hexamer in the asymmetric unit, shares the overall fold and oligomerization state of the wild-type protein, yet superposition of the wild-type and mutant enzyme structures results in relatively high rmsd values for C_α atoms. For alignment of monomers, the range of rmsd is between 1.3 and 1.4 Å, and for one pair, the value is 1.9 Å (comparing molecule A of D44A HI0827 in the coordinates deposited in the PDB). Using the superposition matrix obtained for a monomer to compare wild-type and mutant protein dimers, a large discrepancy is observed between respective positions of the second molecule, with overall dimer rmsd values ranging

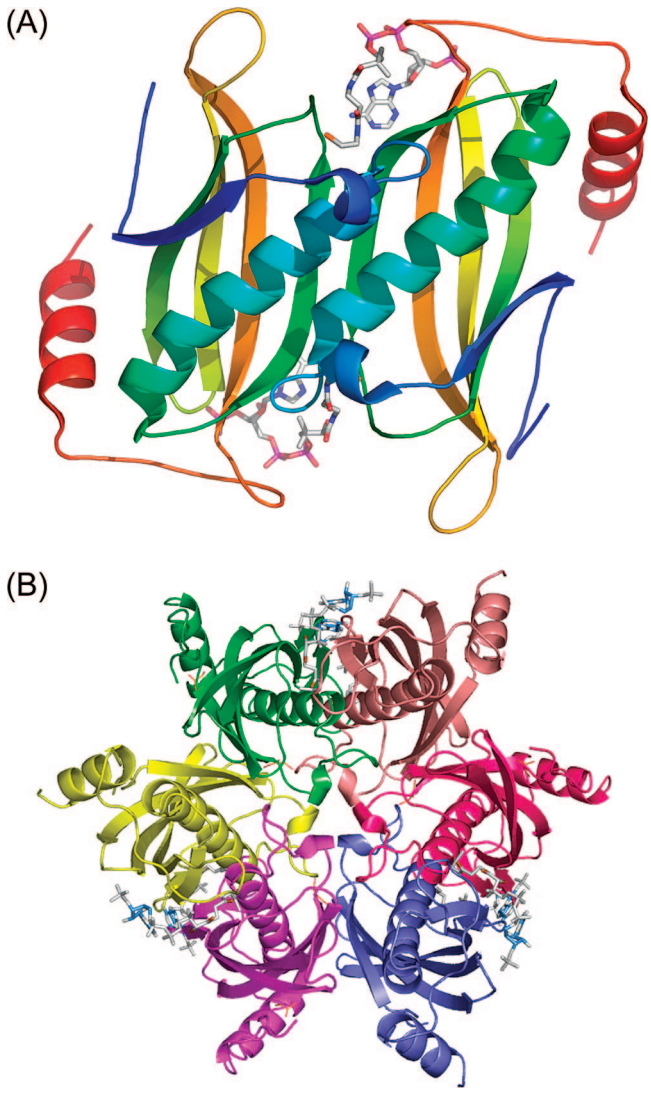

FIGURE 1: Structure of HI0827. (A) Ribbon diagram of the dimeric hot dog fold with the bound CoA molecules. The coloring shows the progression of the polypeptide chains from the N-termini (blue) to the C-termini (red). The CoA molecules are shown with bonds colored according to element type: gray for carbon, blue for nitrogen, red for oxygen, orange for sulfur, and magenta for phosphorus. (B) Ribbon diagram of the biologically relevant hexamer that comprises a trimer of the hot dog dimers.

between 1.9 and 2.4 Å. The rmsd value for superposition of C_α atoms of the entire hexamers is 2.7 Å.

Acyl-CoA Binding Site. For clarity, the two dimer subunits are labeled A and B in the following discussion. Each dimer of wild-type HI0827 contains two symmetrically equivalent active site channels at the dimer interface (Figure 1A). Well-defined electron density corresponding to CoA, the thioesterase substrate hydrolysis product, is present in one of these active sites (Figure 2). The CoA molecule remained bound to the protein through all the purification steps. The second active site contains weaker electron density. This CoA molecule was refined with half-occupancy, giving rise to crystallographic temperature factors on the same order of magnitude as those of the CoA molecule refined with full occupancy. It is impossible to ascertain whether the bound CoA was generated by hydrolysis of a true HI0827 substrate or whether it originated from the CoA cellular pool in *E. coli* generated by other enzymes.

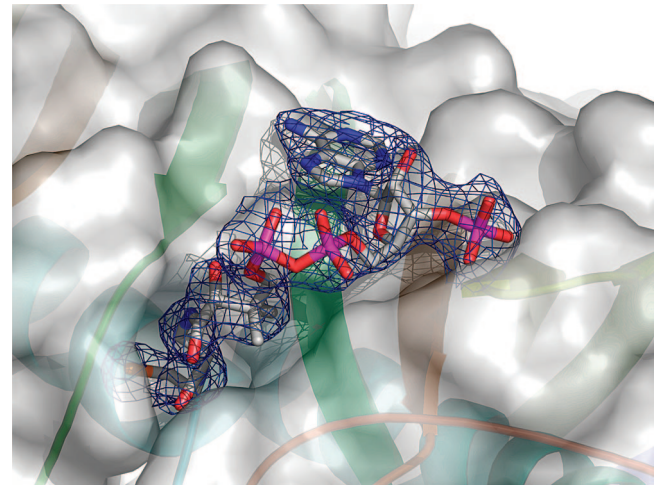

FIGURE 2: CoA binding site. The protein molecular surface is displayed as a semitransparent surface covering a ribbon diagram of HI0827. The solvent-modified experimental electron density for the fully occupied CoA molecule is shown as a blue mesh and is contoured at the 1σ level. The atom coloring is the same as in Figure 1.

The adenine groups of the high-occupancy CoA molecule and a crystallographic symmetry-related molecule stack against one another through crystal packing interactions, which is unlikely to be a biologically relevant association; indeed, CoA molecules bind in similar orientation but without the base stacking interactions across hexamers in the two other hexameric thioesterase structures that were determined by the structural genomics centers (PDB entries 1VPM and 1Y7U). As with HI0827, the CoA must bind to these enzymes tightly because the molecules were retained through the purification process. We note that the 1VPM structure contains four CoA molecules, whereas the active sites of two other subunits are unoccupied. For 1Y7U, CoA occupies all active sites.

Each CoA molecule binds at the dimer interface and over the β-sheet edge. One side of the CoA is flanked by part of a loop on monomer A that connects the C-terminal β-strand to the C-terminal α-helix (residues 125–131). The nucleotide moiety of the CoA is largely exposed to solvent above the β-sheet, whereas the pantethenate and the β-mercaptoethylamine units are wedged at the interface between the two monomers (Figure 3A). The 3′-phosphoryl group of the CoA ribose forms intricate electrostatic interactions with the backbone amide groups of Arg90, Ser91, and Ser92 of molecule A, as well as with the hydroxyl groups of Ser91 and Ser92 (Figure 3A). An alignment of HI0827 sequence homologues that share >50% identity indicates that Ser62 is invariant whereas Ser91 is frequently replaced with a threonine. The guanidinium group of molecule A's Arg90 is located nearby, exhibiting two alternate conformations, none of which forms a salt bridge with the 3′-phosphoryl group of the ribose. Arg90 is not conserved. Other interactions of the nucleotide unit include the adenine amino group interacting with the Asn68 side chain of molecule B, the 5′ α-phosphate interacting with Ser131 hydroxyl group of molecule A, and the β-phosphate interacting with a calcium ion (present in the crystallization solution but not considered physiologically relevant). Neither Asn68 nor Ser131 is conserved.

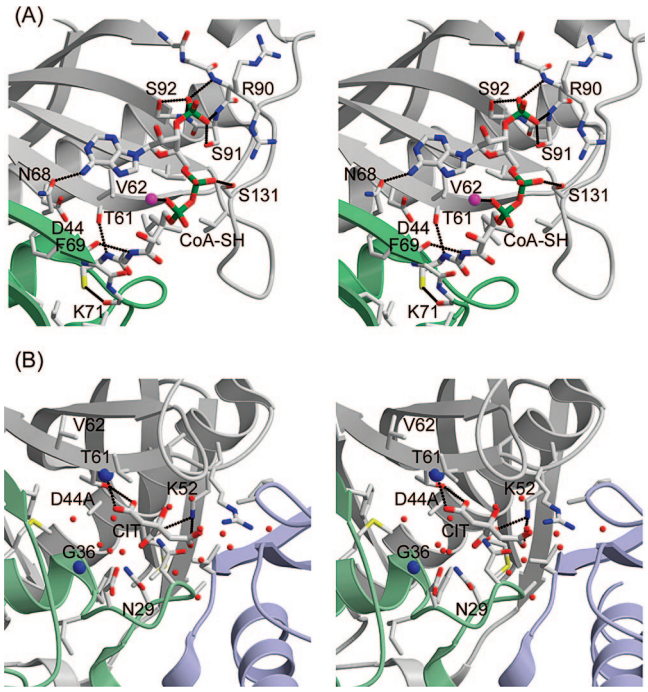

FIGURE 3: Stereoscopic representation of atomic interactions associated with the substrate binding site. (A) Key interactions of CoA bound to wild-type HI0827. Atomic coloring is as follows: gray for carbon, blue for nitrogen, red for oxygen, yellow for sulfur, green for phosphorus, magenta for calcium, and red spheres for water molecules. The two colors (gray and light green) of the ribbon trace correspond to the two molecules within the dimer. (B) Environment of the bound citrate corresponding to the binding site for the substrate's acyl group. In addition to the gray and light green ribbons of the dimer's subunits, the light blue ribbon corresponds to a subunit of a neighboring dimer that also flanks the acyl chain binding site.

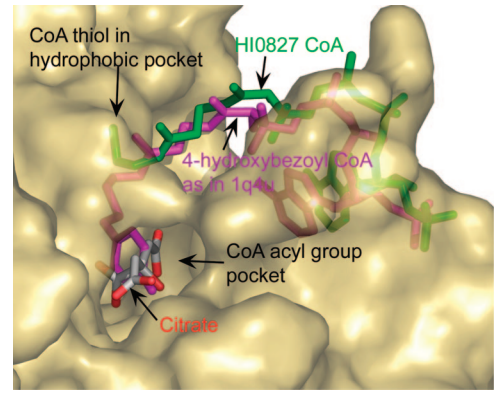

FIGURE 4: Substrate binding channel of HI0827 shown in the context of the molecular surface of the D44A mutant. The citrate molecule is colored by element (gray for carbon and red for oxygen), and the CoA is colored green. The location of the CoA was obtained by superposing wild-type HI0827 and the mutant structures. Also shown is the 4-hydroxybenzyl-CoA inhibitor (colored magenta) from the structure of 4-hydroxybenzoyl-CoA thioesterase from *Pseudomonas* sp. CBS3 (PDB entry 1Q4U) aligned on D44A HI0827, to demonstrate the similarity in the location of the two binding sites.

The preceding paper (*3*) shows that the interactions described above represent those occurring in solution (*3*). (1) The ^{31}P NMR of the HI0827−CoA complex shows broadening of the 3′-P and 5′-PP peaks, indicating that these groups are pinned to the enzyme surface and do not experience free rotation in solution. That the environment of the 3′-P peak is distinct from solvent is evident from the 0.8 ppm downfield shift observed in the signal of this group. In contrast, the 5′-PP peak engages in fewer interactions, and accordingly, its ^{31}P NMR signals are not shifted. (2) The role of the nucleotide unit in substrate recognition is evident from the 1000-fold difference in the k_{cat}/K_m value measured for butyryl-CoA ($k_{cat}/K_m = 1 \times 10^5$ M^{-1} s^{-1}) in contrast to butyrylpantatheine phosphate ($k_{cat}/K_m = 1 \times 10^2$ M^{-1} s^{-1}) and the 84-fold difference in k_{cat} ($k_{cat} = 6.7$ s^{-1} vs 0.08 s^{-1}).

The methyl groups of the pantethenate unit interact with several hydrophobic residues on molecule A [Val60 (replaced with Ala in some sequences), Val62 (replaced with Ile in some sequences), Val123 (conserved), and Val125 (replaced with Ile in some sequences)], whereas the peptide amide groups form hydrogen bonds, one with a backbone carbonyl group on molecule A (Thr61) and the second with a backbone carbonyl group on molecule B (Phe69). The CoA's thiol group is tucked in a small hydrophobic pocket formed by molecule B (pale green ribbon in Figure 3A). Ile39 (replaced with Leu), Phe69 (conserved), Ile73 (replaced with Val), and Val115 (replaced with Ala) delineate this pocket, which is too small to accommodate a CoA acyl group extension. The CoA thiol forms a hydrogen bond with the backbone C=O group of Lys71. Except for the position of the thiol group, the conformation of the CoA is similar to that seen in the complex between 4-hydroxybenzoyl-CoA thioesterase from *Pseudomonas* sp. CBS-3 and its inhibitor, 4-hydroxyphenacyl-CoA (*26*) (Figure 4). The conformation of the CoA unit is determined by the C-terminal extension, which is present in both HI0827 and the 4-hydroxybenzoyl-CoA thioesterase from *Pseudomonas* sp. CBS3 but not present in the 4-hydroxybenzoyl-CoA thioesterase from *Arthrobacter* sp. strain SU (for further details, see ref *19*). The anchoring of the thiol moiety in the hydrophobic pocket may be responsible in part for the apparent high affinity of CoA for the hexameric acyl-CoA thioesterases. The thiol moiety is buried in the same manner also in the *B. halodurans* and *B. cereus* acyl-CoA thioesterase structures.

The X-ray structure of the HI0827−CoA complex indicates that the desulfoCoA inhibition constant [$K_i = 0.33$ μM (*3*)] is likely to be an underestimate of the CoA binding affinity because the desulfoCoA does not contain the sulfur atom which tucks into a hydrophobic pocket where it engages in formation of a hydrogen bond with the Lys71 backbone C=O group. Moreover, the preceding paper (*3*) shows that CoA directs substrate recognition: (i) CoA binds tighter to the enzyme than does the substrate as implied from the strong feedback inhibition which is evident from the fact that CoA outcompetes the substrate for the enzyme when there is more substrate present then CoA ($K_i \ll K_m$). (ii) CoA binds tighter than substrate analogues [K_i determined for 4-hydroxyphenacyl-CoA (5.8 ± 0.3 μM) and K_i determined for hexyl-CoA ($K_i = 1.9 \pm 0.2$ μM)]. (iii) Despite the dramatic difference in the structures of these inhibitors in the region corresponding to the acyl-thioester unit, their K_i values are similar. The placing of the CoA thiol group in the hydrophobic pocket provides the structural rationale for these kinetic data. Product inhibition is expected to be operative also in the other three hexameric acyl-CoA thioesterases whose structures were

Table 2: Steady State Kinetic Constants for *H. influenzae* HI0827 Mutant D44A and N29A-Catalyzed Hydrolysis of Acyl-CoA Thioesters at pH 7.5 and 25 °C Determined Using the 5,5′-Dithiobis(2-nitrobenzoic acid)-Coupled Spectrophotometric Assay Described in ref *3*

	isobutyryl-CoA			lauroyl-CoA		
	k_{cat} (s^{-1})	K_m (μM)	k_{cat}/K_m (M^{-1} s^{-1})	k_{cat} (s^{-1})	K_m (μM)	k_{cat}/K_m (M^{-1} s^{-1})
wild-type	138 ± 4	13 ± 1	1.1×10^7	9.2 ± 0.3	6.6 ± 0.7	1.4×10^6
D44A mutant	<0.001	ND	ND	<0.001	ND	ND
N29A mutant	2.34 ± 0.04	92 ± 4	2.5×10^4	2.57 ± 0.04	4.2 ± 0.3	6.1×10^5

determined with intrinsic CoA (the enzymes from *B. halodurans* and *B. cereus* and acyl-CoA thioesterase 7 from mouse).

The structural adjustment that must follow substrate hydrolysis may be contrasted with the properties of other hot dog acyl-CoA thioesterases. CoA is not a feedback inhibitor of the 4-hydroxybenzoyl-CoA thioesterases from *Arthrobacter* sp. strain SU and *Pseudomonas* sp. strain CBS3: for CoA $K_i = 29$ and 370 μM, respectively, and for substrate $K_m = 1.2$ and 6.0 μM, respectively. Substrate analogues also bind tighter than CoA (4-hydroxyphenacyl-CoA and 4-hydroxybenzyl-CoA, for *Arthrobacter*, 0.003 and 0.6 μM, respectively, and for *Pseudomonas*, 1.4 and 0.26 μM, respectively).

As there is no space to accommodate an acyl group in the pocket that surrounds the thiol group, the thiol group of an intact substrate must flip and bind such that the acyl group is located in an elongated depression that is solvent accessible. The site's location is analogous to the one that accommodates the 4-hydroxyphenacyl group when the inhibitor binds to the 4-hydroxybenzoyl-CoA thioesterases from *Pseudomonas* sp. CBS-3 and *Arthrobacter* sp. strain SU (*26*) (Figure 4) and to those in other acyl-CoA thioesterases, except that the site shape and residue composition differ in each case. For example, the pocket that accommodates the 4-hydroxyphenacyl group in the structure of the enzyme from *Pseudomonas* is inaccessible to solvent, whereas in the crystal structure of wild-type HI0827, the depression appears only partially buried by a salt bridge between Arg58 on molecule A and Asp33 on molecule B (both conserved in the HI0827 sequence family). Interestingly, this salt bridge is eliminated in the structure of D44A HI0827 described below, where the depression is fully exposed to solvent. The combination of the open acyl-binding site and the tight binding of the CoA unit might explain how the enzyme can efficiently bind and hydrolyze acyl-CoA substrates that have acyl groups of vastly different size, shape, and polarity (*3*).

Residues 58–61 and 125–131 and the side chain of Lys52 of molecule A and residues 29–35 of molecule B line the sides of the depression that accommodates the acyl chain. Notable among these is Asn29 (see below). Residues 44–48 of molecule A are located at the bottom of this depression. Most significant is the invariant Asp44, which functions as the key catalytic residue (see below). A third molecule belonging to a neighboring dimer contributes a few residues to the acyl chain binding site: Leu22, Gly76, and Ala105 (Figure 3B).

The CoA binding channel narrows close to the postulated precleavage position of the thioester group, and presumably after cleavage, the thiol group moves into the hydrophobic pocket. At the neck of the channel, the backbone amide groups of Gly36 on molecule B and Thr61 on molecule A face one another, separated by a distance of 5.4 Å. This arrangement brings the carboxylate group of Asp44 within hydrogen bonding distance of the Thr61 hydroxyl group and the Gly37 backbone amide NH group. In contrast, the "neck" observed in other acyl-CoA thioesterases of known structure is significantly wider. For example, the equivalent amide groups in the 4-hydroxybenzoyl-CoA thioesterases from *Pseudomonas* sp. CBS-3 (*26*), *Arthrobacter* sp. SU (*21, 26*), *E. coli* thioesterase II (*20*), and the PaaI acyl-CoA thioesterase from *Thermus thermophilus* (*27*) are separated by 7.3–8.3 Å. As described below, the neck observed in the structure of the D44A HI0827 mutant structure is in an open conformation.

Structural Differences between Wild-Type and D44A HI0827. The structure analysis confirmed that the key catalytic residue is Asp44, which was suggested by the sequence alignment analysis. Indeed, replacement of Asp44 with Ala results in a dramatic loss of catalytic activity (Table 2). The crystallographic studies of D44A HI0827 were undertaken because the inactive mutant appeared suitable for cocrystallization or soaking experiments. So far, all experiments failed to reveal binding of CoA to the mutant enzyme or of various acyl-CoA compounds that were selected from the set of substrates described in the preceding paper (*3*). Nevertheless, the structure of the mutant enzyme exhibits substantial conformational differences from the structure of the wild-type enzyme. These differences provide insight into the conformational flexibility of HI0827, and the potential for allosteric regulation (see below).

Without bound CoA, the loops in the vicinity of the CoA binding site assume a different conformation. In addition, a seemingly subtle change in the β-strand arrangement at the dimer interface leads to a cumulative discrepancy in the dimer alignment, and consequently in the overall hexameric structure. The β-sheet hydrogen bonding pattern at the subunit interface is perturbed in both structures but in different manners (Figure 5). For each monomer in the mutant protein structure, a β-bulge (*28*) is formed on the β-strand facing the dimer interface, creating a hump in the center of the dimer-spanning β-sheet. The β-bulge in one monomer (labeled B in Figure 5B) conforms to the definition of a classic bulge and includes Glu65 and Ser66 on the external β-strand, and Val119 on the adjacent strand, with Glu65 adopting a helical conformation (*28*). The β-bulge in the second monomer (labeled A in Figure 5B) conforms to the definition of a wide bulge and includes Ser66 and Met67 on the external β-strand, and Ala118 on the adjacent strand, with Ser66 in the left-handed helical conformation. Together, the two bulges perturb the β-sheet hydrogen bonding pattern across the dimer interface. At the level of the hexamer, the 3-fold symmetry of D44A HI0827 is imperfect because as a rotation around the 3-fold symmetry axis is made, the arrangement of paired β-bulges in two dimers obeys the

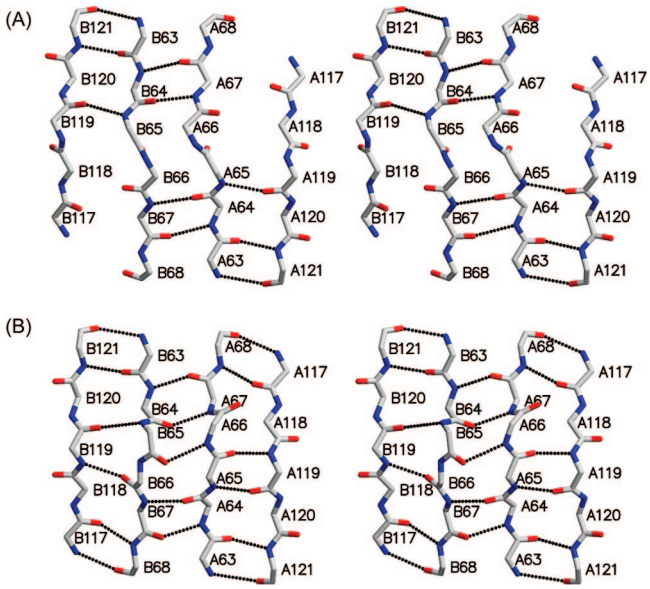

FIGURE 5: Stereoscopic representation of interface β-sheet interactions in wild-type (A) and D44A (B) HI0827. Residues are numbered, and the letters A and B correspond to the two dimer's subunits.

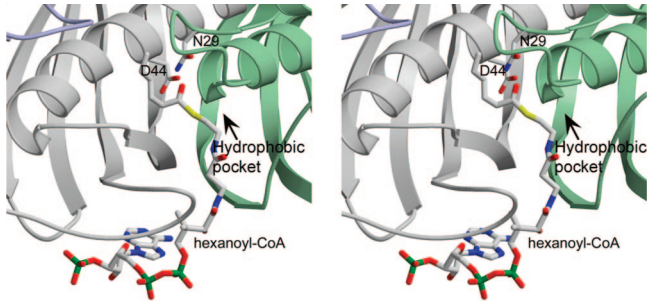

FIGURE 6: Stereoscopic representation of a model of hexanoyl-CoA bound to wild-type HI0827. Coloring as in Figure 3. The side chains of Asp44 and Asn29 projecting toward the opposite faces of the substrate's thioester CO group are shown.

3-fold symmetry whereas in the third dimer the order of classic versus wide bulge is reversed.

The wild-type HI0827 hexamer obeys the perfect 3-fold crystallographic symmetry of the tetragonal $I4_132$ space group. The interface's β-strands do not contain bulges. Instead, the β-sheet hydrogen bond interaction pattern is perturbed in the same manner in both molecules (Figure 5A): the Glu65 NH group is hydrogen-bonded to Val119 O, after which the Glu65 dihedral angles lead to a twist of the β-strand such that the CO group and the Asn68 NH and CO groups do not form β-sheet interactions with the adjacent intramolecular β-strand. This arrangement can be viewed as an incomplete bulge which prevents the repair of the β-sheet hydrogen bond pattern beyond the perturbation. The "tearing apart" of the β-sheet may be functionally relevant because it brings the side chain of Asn68 close to CoA for electrostatic interaction between the adenine amino group and the side chain CO group of Asn68 (Figure 3A). We note that the same β-sheet distortion is seen in the two other hexameric acyl-CoA thioesterases (PDB entries 1VPM and 1Y7U), where the CoA adenine amino group interacts with the side chain of an aspartic acid positioned in a manner equivalent to that of the Asn68 side chain. In contrast, the β-sheet hydrogen bonding pattern in the nonhexameric acyl-CoA thioesterase structures is not perturbed.

The reorganization of the β-strands at the interface affects the hydrophobic niche where the CoA thiol group binds (or vice versa). As discussed above, the thiol group forms only one polar interaction with the backbone carbonyl of Lys71. In D44A HI0827, a water molecule binds in a position equivalent to that of the CoA thiol group and the hydrophobic niche has become more hydrophilic in nature. Both main chains and side chains have changed so that in addition to the backbone carbonyl of Lys71, the water molecule also interacts with the hydroxyl group of Thr116 and the backbone carbonyl oxygen atom of Val115.

As detailed above, protomer A of the D44A HI0827 structure deviates most from its counterpart in the wild-type structure. This may be due to the presence of a citrate molecule (present in the crystallization solution) near one of the active sites at the protomer A−protomer B interface (Figure 3B). The other five active site pockets do not contain any bound ligand, and although they exhibit structural differences relative to the wild-type enzyme, these are not as large as observed in protomer A.

The citrate ligand is bound at the location where the substrate acyl chain is expected to bind (Figure 4). The citrate ligand forms only a few interactions with protein groups, and it is surrounded by many water molecules (Figure 3B). Thus, the citrate binding is most likely to be incidental (notably, citrate is not an inhibitor). Nevertheless, the change in the conformation of the "acyl group-binding site" that is observed in the citrate-bound D44A HI0827 protomer suggests binding site plasticity that might be important for the accommodation of substrate acyl moieties that are different in size, shape, and polarity. For example, the distance between the two backbone amide groups of Thr61 (molecule A) and Gly36 (molecule B) at the entrance to the acyl chain pocket in D44A HI0827 is 8.3 Å rather than the distance of 5.4 Å observed in the wild-type enzyme. In the mutant enzyme protomers, where the acyl chain binding sites are devoid of bound citrate, the corresponding distance ranges between 7.1 and 8.0 Å, also significantly larger than the distance in the wild-type enzyme. Currently, it is impossible to ascertain whether the absence of CoA leads to these differences or whether the removal of the Asp44 carboxylate in the D44A mutant induces the conformational change: Asp44 interacts with molecule A's Thr61 hydroxyl group (2.5 Å) and with the backbone amide of molecule B's Gly37 (2.9 Å). A replacement with an alanine eliminates these interactions and may result in greater flexibility of the polypeptide segments that delineate the binding pocket. The exact size of the pocket upon binding of intact acyl-CoA substrate is unknown; nevertheless, in both structures, the crevice is sufficiently wide to accommodate branched acyl chains. This is consistent with the substrate screening results described in the preceding paper (*3*). Moreover, a widening of the thioester acyl chain binding site may have a functional role in wild-type HI0827 because substrate binding is likely to perturb the interactions of Asp44 with Thr61 and Gly37.

Model of Acyl-CoA Binding and Identification of Catalytic Residues. The size of the acyl chain pocket suggests a short acyl group extension, but the shape and environment do not shed light on the exact chemical nature of the chain. The preceding paper (*3*) describes the activity studies that

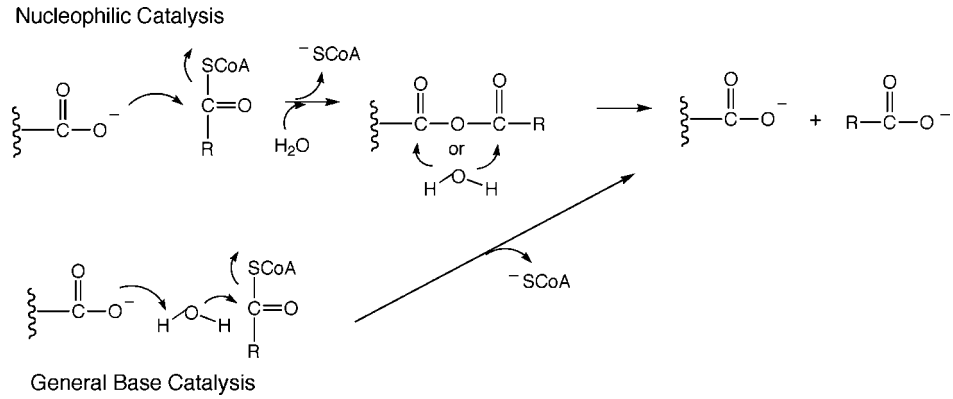

FIGURE 7: Two alternative catalytic mechanisms of HI0827.

identified a wide spectrum acyl-CoA compounds that the enzyme hydrolyzes efficiently with k_{cat}/K_m values ranging between $\sim 10^3$ and $\sim 10^8$ M^{-1} s^{-1} (*3*). The best substrates span a broad range of chemical character. Some examples are phenylacetyl-CoA ($k_{cat}/K_m = 8.3 \times 10^7$ M^{-1} s^{-1}), glutaryl-CoA ($k_{cat}/K_m = 1.3 \times 10^7$ M^{-1} s^{-1}), isobutyryl-CoA ($k_{cat}/K_m = 1.1 \times 10^7$ M^{-1} s^{-1}), and lauroyl-CoA ($k_{cat}/K_m = 1.4 \times 10^6$ M^{-1} s^{-1}). These substrates may be readily docked in the active site of wild-type HI0827. Figure 6 shows a model for the binding of hexanoyl-CoA, a substrate that HI0827 hydrolyzes with a k_{cat}/K_m of 3.6×10^6 M^{-1} s^{-1}. The hexanoyl group was taken from the structure of *T. thermophilus* acyl-CoA thioesterase bound to hexanoyl-CoA (*27*). The CoA conformation is as seen in wild-type HI0827 except that the β-mercaptoethyl moiety was rotated toward the postulated acyl chain binding channel and the conformation of the aliphatic moiety of the hexanoyl group was modified to generate hydrophobic contacts with protein groups. The thioester's carbonyl carbon atom faces Asp44 on one side and Asn29 of the mate molecule on the opposite side. The carbonyl oxygen atom is oriented toward the conserved Gly36 amide (located at the N-terminus of the α-helix in subunit B) by analogy to the orientation of the carbonyl group in the structures of the *Pseudomonas* sp. CBS-3 and *Arthrobacter* 4-hydroxybenzoyl-CoA thioesterases in complexes with inhibitors (*21, 26*). The backbone amide NH group of this N-terminus residue engages in hydrogen bond interaction with the substrate thioester, thereby orienting and polarizing the C═O group for nucleophilic attack (*29*). This is the only conserved element of the hot dog thioesterase catalytic motif. Because the binding site may undergo conformational change, the extent of which is unpredictable, minimization was meaningless. This is by no means an accurate model. It is intended to broadly indicate the location of the substrate. Indeed, it is clear from the size of the acyl chain binding pocket that the selected conformation of the aliphatic chain is only one of many possible conformations.

The mechanism of the hot dog acyl-CoA thioesterases has been much discussed in terms of nucleophilic attack by a carboxyl group of an aspartate/glutamate to form an acyl−enzyme intermediate, or an alternative mechanism involving nucleophilic attack of the hydrolytic water molecule aided by the carboxylate group, which in this case serves as the general base (*20, 21, 26, 27*) (Figure 7). Because of the inherent inaccuracy in modeling the HI0827−acyl-CoA complex and the expected change in conformation upon substrate binding, the orientation of the modeled substrate's thioester carbonyl and its distance from Asp44 carboxylate group are also inaccurate. Hence, we are unable to distinguish between the nucleophilic attack and general base mechanisms based on such a model and await a structure determination with an uncleaved substrate or a substrate analogue. Single-turnover ^{18}O labeling experiments may help resolve this issue.

A remarkable feature of the hot dog thioesterase family is that the catalytic carboxylate residue is found in either one of two positions on the catalytic scaffold. This divergence of the catalytic motif, which divides the family along two evolutionary branches, was originally discovered by the structure–function analysis of the two prototypes: *Arthrobacter* sp. strain SU 4-hydroxybenzoyl-CoA thioesterase and *Pseudomonas* sp. strain CBS3 4-hydroxybenzoyl-CoA thioesterase. Here we note that Asp44 of HI0827 occupies the same position as the catalytic Glu73 of the *Arthrobacter* 4-hydroxybenzoyl-CoA thioesterase (i.e., the center of the α-helix of protomer A) whereas Asn29 of HI0827 occupies the same position as the catalytic Asp17 of the *Pseudomonas* 4-hydroxybenzoyl-CoA thioesterase (i.e., the loop that connects to the N-terminus of the protomer B α-helix). Thus, HI0827 is of the same lineage as the *Arthrobacter* 4-hydroxybenzoyl-CoA thioesterase. Whereas Asp44 of HI0827 is essential for catalysis, the conserved residue Asn29, located on the opposite face of the substrate thioester group, makes a much smaller contribution (Table 2). This same behavior has been reported for the corresponding Glu73/Gln58 pair in the *Arthrobacter* 4-hydroxybenzoyl-CoA thioesterase (*19, 30*) and Asp75/Asn60 pair in the *E. coli* phenylacetyl-CoA thioesterase PaaI (*27*).

Allosteric Regulation? It is tempting to speculate that HI0827 may be subject to allosteric regulation because the different occupancies of the two CoA molecules observed in the crystal structure of the wild-type enzyme may arise from different binding affinities and because of the enzyme's potential to form two alternative subunit−subunit interactions within a dimer. Clearly, this proposal needs to be confirmed experimentally. Nevertheless, one may envisage a sequential hydrolytic cycle in which an acyl-CoA substrate molecule binds in one site within a dimer while the second site is blocked by a tightly bound CoA molecule. Acyl-CoA binding in the first site could lead to structural changes that propagate to the CoA-bound site, perhaps by changing the hydrogen bonding pattern along the interface β-strands, which in turn reduces the affinity for the tightly bound CoA molecule. Upon hydrolysis of the acyl-CoA, the free ethylthiol group

flips and anchors in the hydrophobic pocket. At the same time, the CoA molecule released from the mate site enables binding of a new substrate molecule. The cycle of events within a dimer may also be coordinated across the trimeric ring because the neighboring dimer participates in formation of the binding site of the substrate's acyl chain. This proposal awaits experimental confirmation.

ACKNOWLEDGMENT

We thank the S2F Structural Genomics team for discussions and Eugene Melamud and John Moult for their work on the S2F bioinformatics web site (http://s2f.carb.nist.gov). We thank the staff of the IMCA-CAT beamlines at the Advanced Photon Source (APS) for their assistance with data collection. The IMCA-CAT facility is supported by companies of the Industrial Macromolecular Crystallographic Association, through a contract with the Illinois Institute of Technology. Use of the APS was supported by the U.S. Department of Energy, Basic Energy Sciences, Office of Science, under Contract W-31-109-Eng-38.

REFERENCES

1. Leesong, M., Henderson, B. S., Gillig, J. R., Schwab, J. M., and Smith, J. L. (1996) Structure of a dehydratase-isomerase from the bacterial pathway for biosynthesis of unsaturated fatty acids: Two catalytic activities in one active site. *Structure 4*, 253–264.
2. Altschul, S. F., Madden, T. L., Schaffer, A. A., Zhang, J., Zhang, Z., Miller, W., and Lipman, D. J. (1997) Gapped BLAST and PSI-BLAST: A new generation of protein database search programs. *Nucleic Acids Res. 25*, 3389–3402.
3. Zhuang, Z., Song, F., Zhao, S., Li, L., Cau, J., Eisenstein, E., Herzberg, O., and Dunaway-Mariano, D. (2008) Divergence of Function in the Hot Dog Fold Enzyme Superfamily: The Bacterial Thioesterase YciA. *Biochemistry 47*, 2789–2796.
4. Willis, M. A., Song, F., Zhuang, Z., Krajewski, W., Chalamasetty, V. R., Reddy, P., Howard, A., Dunaway-Mariano, D., and Herzberg, O. (2005) Structure of YciI from *Haemophilus influenzae* (HI0828) reveals a ferredoxin-like α/β-fold with a histidine/aspartate centered catalytic site. *Proteins 59*, 648–652.
5. Erlich, H. A. (1992) *PCR Technology Principles and Applications for DNA Amplification*, Freeman and Co., New York.
6. Otwinowski, Z., and Minor, W. (1997) Processing of X-ray diffraction data collected in oscillation mode. *Methods Enzymol. 276*, 307–326.
7. Terwilliger, T. C., and Berendzen, J. (1999) Automated MAD and MIR structure solution. *Acta Crystallogr. D55*, 849–861.
8. Terwilliger, T. C. (2000) Maximum-likelihood density modification. *Acta Crystallogr. D56*, 965–972.
9. Jones, T. A., Zou, J. Y., Cowan, S. W., and Kjeldgaard, M. (1991) Improved methods for binding protein models in electron density maps and the location of errors in these models. *Acta Crystallogr. A47*, 110–119.
10. Brunger, A. T., Adams, P. D., Clore, G. M., DeLano, W. L., Gros, P., Grosse-Kunstleve, R. W., Jiang, J. S., Kuszewski, J., Nilges, M., Pannu, N. S., Read, R. J., Rice, L. M., Simonson, T., and Warren, G. L. (1998) Crystallography & NMR system: A new software suite for macromolecular structure determination. *Acta Crystallogr. D54*, 905–921.
11. Murshudov, G. N., Vagin, A. A., and Dodson, E. J. (1997) Refinement of macromolecular structures by the maximum-likelihood method. *Acta Crystallogr. D53*, 240–255.
12. Collaborative Computational Project Number 4 (1994) The CCP4 suite: Programs for protein crystallography. *Acta Crystallogr. D50*, 760–763.
13. Winn, M. D., Isupov, M. N., and Murshudov, G. N. (2001) Use of TLS parameters to model anisotropic displacements in macromolecular refinement. *Acta Crystallogr. D57*, 122–133.
14. Laskowski, R. A., Macarthur, M. W., Moss, D. S., and Thornton, J. M. (1993) PROCHECK: A Program to Check the Stereochemical Quality of Protein Structures. *J. Appl. Crystallogr. 26*, 283–291.
15. Hooft, R. W., Vriend, G., Sander, C., and Abola, E. E. (1996) Errors in protein structures. *Nature 381*, 272.
16. Nicholls, A., Bharadwaj, R., and Honig, B. (1993) Grasp: Graphical Representation and Analysis of Surface Properties. *Biophys. J. 64*, A166–A166.
17. Kraullis, P. J. (1991) A program to produce both detailed and schematic plots of protein structures. *J. Appl. Crystallogr. 24*, 946–950.
18. Merritt, E. A., and Bacon, D. J. (1997) Raster3D: Photorealistic molecular graphics. *Methods Enzymol. 277*, 505–524.
19. Benning, M. M., Wesenberg, G., Liu, R., Taylor, K. L., Dunaway-Mariano, D., and Holden, H. M. (1998) The three-dimensional structure of 4-hydroxybenzoyl-CoA thioesterase from *Pseudomonas* sp. strain CBS-3. *J. Biol. Chem. 273*, 33572–33579.
20. Li, J., Derewenda, U., Dauter, Z., Smith, S., and Derewenda, Z. S. (2000) Crystal structure of the *Escherichia coli* thioesterase II, a homolog of the human Nef binding enzyme. *Nat. Struct. Biol. 7*, 555–559.
21. Thoden, J. B., Zhuang, Z., Dunaway-Mariano, D., and Holden, H. M. (2003) The structure of 4-hydroxybenzoyl-CoA thioesterase from *Arthrobacter* sp. strain SU. *J. Biol. Chem. 278*, 43709–43716.
22. Forwood, J. K., Thakur, A. S., Guncar, G., Marfori, M., Mouradov, D., Meng, W., Robinson, J., Huber, T., Kellie, S., Martin, J. L., Hume, D. A., and Kobe, B. (2007) Structural basis for recruitment of tandem hotdog domains in acyl-CoA thioesterase 7 and its role in inflammation. *Proc. Natl. Acad. Sci. U.S.A. 104*, 10382–10387.
23. Tajika, Y., Sakai, N., Tanaka, Y., Yao, M., Watanabe, N., and Tanaka, I. (2004) Crystal structure of conserved protein PH1136 from *Pyrococcus horikoshii*. *Proteins 55*, 210–213.
24. Kimber, M. S., Martin, F., Lu, Y., Houston, S., Vedadi, M., Dharamsi, A., Fiebig, K. M., Schmid, M., and Rock, C. O. (2004) The structure of (3R)-hydroxyacyl-acyl carrier protein dehydratase (FabZ) from *Pseudomonas aeruginosa*. *J. Biol. Chem. 279*, 52593–52602.
25. Kostrewa, D., Winkler, F. K., Folkers, G., Scapozza, L., and Perozzo, R. (2005) The crystal structure of PfFabZ, the unique β-hydroxyacyl-ACP dehydratase involved in fatty acid biosynthesis of *Plasmodium falciparum*. *Protein Sci. 14*, 1570–1580.
26. Thoden, J. B., Holden, H. M., Zhuang, Z., and Dunaway-Mariano, D. (2002) X-ray crystallographic analyses of inhibitor and substrate complexes of wild-type and mutant 4-hydroxybenzoyl-CoA thioesterase. *J. Biol. Chem. 277*, 27468–27476.
27. Kunishima, N., Asada, Y., Sugahara, M., Ishijima, J., Nodake, Y., Miyano, M., Kuramitsu, S., and Yokoyama, S. (2005) A novel induced-fit reaction mechanism of asymmetric hot dog thioesterase PAAI. *J. Mol. Biol. 352*, 212–228.
28. Richardson, J. S., Getzoff, E. D., and Richardson, D. C. (1978) The beta bulge: A common small unit of nonrepetitive protein structure. *Proc. Natl. Acad. Sci. U.S.A. 75*, 2574–2578.
29. Zhuang, Z., Song, F., Zhang, W., Taylor, K., Archambault, A., Dunaway-Mariano, D., Dong, J., and Carey, P. R. (2002) Kinetic, Raman, NMR, and site-directed mutagenesis studies of the *Pseudomonas* sp. strain CBS3 4-hydroxybenzoyl-CoA thioesterase active site. *Biochemistry 41*, 11152–11160.
30. Song, F. (2006) Structure, function and mechanism in the "hot dog"-fold enzyme superfamily thioesterases, in *Department of Chemistry*, p 50, University of New Mexico, Albuquerque.

BI702336D